

25 **Title:** Comparative Analysis of *Microcystis* Buoyancy in Western Lake Erie and Saginaw Bay of Lake

26 Huron

27

28 **Authors:** Paul A. Den Uyl ^a, Seamus B. Harrison ^a, Casey M. Godwin ^{a*}, Mark D. Rowe ^b, J. Rudi Strickler ^{c,d},
29 and Henry A. Vanderploeg ^b

30 ^a Cooperative Institute for Great Lakes Research, School for Environment and Sustainability, University
31 of Michigan, 440 Church Street, Ann Arbor MI 48109

32 ^b National Oceanic and Atmospheric Administration, Great Lakes Environmental Research Laboratory,
33 4840 South State Road, Ann Arbor MI 48108

34 ^c Department of Biological Sciences, University of Wisconsin-Milwaukee, 600 East Greenfield
35 Avenue, Milwaukee, WI 53204

36 ^d Marine Science Institute, The University of Texas at Austin, 750 Channel View Drive, Port
37 Aransas, TX 78373

38

39

40

41

42 *Corresponding author, cgodwin@umich.edu

43 **Highlights:**

44 • *Microcystis* colonies in western Lake Erie were mostly buoyant

45 • *Microcystis* colonies in Saginaw Bay were mostly sinking

46 • Buoyant and sinking velocities were weakly correlated with colony size

47 • Apparent colony density of small colonies was more variable and responsive to light

48

49 **Abstract**

50 *Microcystis* is the predominant genus of harmful cyanobacterium in both Lake Erie and Saginaw Bay of
51 Lake Huron and has the capacity to regulate the buoyancy of its colonies, sinking under certain
52 conditions while floating towards the surface in others. Understanding the factors that control buoyancy
53 is critical for interpretation of remote sensing data, modeling and forecasting harmful algal blooms
54 within these two systems. To determine if *Microcystis* colony buoyancy in the two lakes responds
55 similarly to diurnal light cycles, colony buoyant velocity (floating/sinking terminal velocity in a quiescent
56 water column) and size were measured after manipulating the intensity of sunlight. Overall, there were
57 more positively buoyant (floating) colonies in Lake Erie while most of the colonies in Saginaw Bay were
58 negatively buoyant (sinking). In Lake Erie the colonies became less buoyant at increased light intensities
59 and were less buoyant in the afternoon than in the morning. In both lakes, apparent colony density was
60 more variable among small colonies (< 200 μ m), whereas larger colonies showed a diminished response
61 of density to light intensity and duration. These findings suggest that colony density becomes less plastic
62 as colonies increase in size, leading to a weak relationship between size and velocity. These relationships
63 may ultimately affect how the bloom is transported throughout each system and will help explain
64 observed differences in vertical distribution and movement of *Microcystis* in the two lakes.

65 **Keywords:** *Microcystis*, buoyancy, vertical migration, Lake Erie, Saginaw Bay

66

67 **1. Introduction**

68 Harmful algal blooms (HABs) are a globally widespread problem in nearshore marine and
69 freshwater ecosystems (Harke et al., 2016; Paerl and Otten, 2013). HABs can cause major disruptions in
70 ecological communities and pose health risks to both animals and humans (Hilborn and Fournie, 2008;
71 Paerl et al., 2001). In the Laurentian Great Lakes of North America, HABs occur as a symptom of
72 eutrophication with likely promotion from invasive dreissenid mussels in western Lake Erie
73 (Vanderploeg et al. 2001, 2002; Stumpf et al., 2012; Watson et al., 2016), Saginaw Bay of Lake Huron
74 (Vanderploeg et al. 2001, 2002; Fishman et al., 2010), and several other locations (Bartlett et al., 2018;
75 Carmichael and Boyer, 2016). In western Lake Erie and Saginaw Bay, HABs are often composed of
76 cyanobacteria of the genus *Microcystis*, which frequently dominates warm, shallow, eutrophic lakes.
77 *Microcystis* is capable of producing toxins called microcystins (Harke et al., 2016; Jöhnk et al., 2008;
78 Paerl et al., 2011) that can affect drinking water quality or lead to recreational contact advisories
79 (www.epa.gov/cyanohabs). Like other phytoplankton, the population dynamics of *Microcystis* are driven
80 principally by light intensity, nutrient availability, predation, and temperature (Harke et al., 2016;
81 Litchman and Klausmeier, 2008). Much of the research on HABs in the Great Lakes has focused on
82 growth and toxicity in response to nutrients (Bertani et al., 2016; Chaffin et al., 2011; Michalak et al.,
83 2013) and trophic interactions, particularly by introduced dreissenid mussels (Vanderploeg et al. 2001,
84 2002, 2009; Johengen et al., 2013; Tang et al., 2014). However, unlike most eukaryotic phytoplankton in
85 the Great Lakes, *Microcystis* exhibits buoyant vertical migration, which allows the genus to exploit
86 gradients in nutrients, light, and consumer abundance that occur with depth in lakes (Reynolds et al.,
87 1987).

88 Although the capacity of phytoplankton to adjust their buoyancy is not unique to cyanobacteria,
89 only cyanobacteria possess gas vesicles which are important to driving buoyancy, and *Microcystis* shows
90 particularly flexible buoyancy regulation. *Microcystis* can form large colonies (i.e. > 1 mm), consisting of
91 ellipsoid cells (~ 5 μ m) in a mucilaginous aggregation, which can achieve buoyant velocities greater than
92 one meter per hour (Nakamura et al., 1993; Wallace and Hamilton, 1999). Buoyancy of *Microcystis* is
93 governed by the size of colonies and their density relative to water (Li et al., 2016; Nakamura et al.,
94 1993; Wu et al., 2020a). Colony size is highly variable (Wu et al., 2020a) and the buoyant velocity (or
95 sinking velocity) for a colony of any size is also influenced by the colony's shape and compactness (Li et
96 al., 2016; Wu et al., 2020a; Zhu et al., 2014a). The density of a colony is determined as a result of the
97 balance between intracellular gas vesicles, which decrease cell density compared to water, and
98 macromolecules and intracellular carbohydrate stores, which increase density of the cell (Konopka et al.,
99 1987; Kromkamp and Mur, 1984; Oliver, 1994; Thomas and Walsby, 1985). Ultimately, the extent of
100 vertical migration by *Microcystis* is governed by changes in colony density and size in combination with
101 the turbulent environment in the water (Hozumi et al., 2019; Wallace et al., 2000; Wallace and
102 Hamilton, 1999).

103 Buoyancy regulation and vertical migration in *Microcystis* are likely adaptations to exploit
104 vertical gradients of light, nutrients, and consumer abundance (Bormans et al., 1999; Reynolds et al.,
105 1987) and may contribute to the competitive advantage of *Microcystis* over eukaryotic phytoplankton in
106 eutrophic conditions (Huisman et al., 2004; Xiao et al., 2018). For example, *Microcystis* biomass can
107 accumulate near the surface under quiescent conditions, forming 'scums' early in the morning and
108 sinking when light intensity increases later in the day (Ibelings et al., 1991b; Reynolds, 1973; Reynolds et
109 al., 1987; Zhu et al., 2014b). This behavior is thought to be an adaptation to obtain sufficient light for
110 photosynthesis, while avoiding damaging effects of high light intensity and short wavelengths at the
111 surface, particularly during mid-day (Reynolds and Walsby, 1975). This pattern is supported by both in

112 situ observations (Ibelings et al., 1991b; Visser et al., 1996) and laboratory experiments (Ibelings et al.,
113 1991a; Visser et al., 1997; Wu et al., 2020b; Xiao et al., 2018) and has been included in mechanistic
114 models (Aparicio Medrano et al., 2013; Chien et al., 2013; Visser et al., 1997; Wallace et al., 2000). The
115 response of *Microcystis* buoyancy to light is a function of both intensity and duration (Wallace and
116 Hamilton, 1999) and is mediated by rapid changes in carbohydrate stores (Konopka et al., 1987; Wallace
117 and Hamilton, 1999; Xiao et al., 2012). Buoyancy regulation has also been proposed as an adaptation for
118 cyanobacteria, including *Microcystis*, to exploit higher inorganic nutrient concentrations in the
119 metalimnion or near the sediments (Fogg and Walsby, 1971). Several laboratory studies have shown
120 that nitrogen (N) or phosphorus (P) limitation can diminish the response of *Microcystis* buoyancy to light
121 (Brookes and Ganf, 2001; Chu et al., 2007; Konopka et al., 1987). While the response of buoyancy to
122 nutrient limitation appears consistent with an adaptation to acquire nutrients at depth, Bormans et al.
123 (1999) argued that the tendency to sink under nutrient stress could be due to low growth rates and
124 stresses that occur under nutrient limitation. Similar to the effects of nutrient limitation, low
125 temperature also decreases buoyancy and increases the tendency for colonies to sink (Thomas and
126 Walsby, 1986; Visser et al., 1995; You et al., 2018).

127 In addition to the ecological significance of buoyancy regulation and vertical migration by
128 *Microcystis*, these phenomena also have important implications for remote sensing, modeling and
129 forecasting of HABs in lakes. Ocean color remote sensing is used to monitor HABs, but assessing total
130 bloom biomass from remote sensing is complicated by the varying vertical distribution of colonies as a
131 function of buoyancy and turbulence (Wynne et al., 2011). Rowe et al. (2016) described a model to
132 predict *Microcystis* vertical distribution as a function of colony size distribution, buoyant velocity, and
133 turbulent diffusivity, and showed improvement in forecasts of bloom trajectory when a model of colony
134 vertical distribution was linked to a three-dimensional hydrodynamic forecast. The model of Rowe et al.
135 (2016), and similar models of phytoplankton vertical distribution (Ross and Sharples, 2004), require

136 input of empirically-measured buoyant velocity. While models have been developed to predict changes
137 in density as a function of light intensity and duration due to changing carbohydrate content (Aparicio
138 Medrano et al., 2013; Ibelings et al., 1991b; Okada and Aiba, 1983, 1986; Visser et al., 1997; Wallace et
139 al., 2000), they still cannot predict all variables that control buoyant velocity and vertical distribution,
140 including gas vesicle volume fraction, the influence of nutrient limitation, and colony size distribution.

141 To date, the vertical migration of buoyant *Microcystis* colonies in the Great Lakes has been
142 studied under a limited set of environmental conditions in western Lake Erie, including both
143 experimental methods and vertical profiles collected in situ (Bosse et al., 2019; Kramer, 2018; Rowe et
144 al., 2016). The aim of the present study was to measure buoyant velocities of colonies as a function of
145 light intensity, time of day, and colony size in western Lake Erie and Saginaw Bay, which have different
146 nutrient loading concentrations and stoichiometry (Johengen et al. 2013). Intact lake water samples
147 were incubated under a range of light intensities in outdoor incubations and microscopic
148 cinematography (micro-cinematography) was used to empirically measure both the size of colonies and
149 their terminal floating or sinking velocity in a quiescent water column (buoyant velocity). We
150 hypothesized that increasing light intensity would cause *Microcystis* colonies to become less buoyant,
151 prolonged exposure to high light intensities would cause colonies to become negatively buoyant, and
152 buoyant velocity would increase with colony size.

153

154

155

156

157

158

159 **2. Methods**

160 2.1 Experimental design overview

161 Short-term incubation experiments were performed with water samples collected from
162 Lake Erie and Saginaw Bay. These experiments were designed to maintain the temperature and
163 other conditions found in the lakes, while manipulating the intensity of sunlight to mimic
164 different depths within the water column. The vertical velocities of colonies were empirically
165 measured after the samples acclimated to these different levels of light intensity and this was
166 repeated in the morning and afternoon to examine the effect of exposure history on buoyancy.
167 The complete details of the experimental setup and analyses are described in the following
168 sections.

169 2.2 Sample collection and processing

170 Samples of whole lake water were collected during the 2016 and 2019 summer bloom
171 seasons in western Lake Erie and during the 2019 season in Saginaw Bay. In 2016, samples were
172 collected at five stations in western Lake Erie between August 29 and October 11 (See Table 1,
173 Gill et al., 2017). During 2016, the stations were selected based on highest abundance of
174 phytoplankton (much of which is *Microcystis*), as quantified by chlorophyll concentration
175 measured using a FluoroProbe fluorometer (bbe Moldaenke). In 2019 the sampling design was
176 adapted to contrast the two lakes and so samples were collected at one station in western Lake
177 Erie (WE2) and one station in Saginaw Bay (SB14), between July 10 and August 12.

178

179

180

181 For all experiments, water was collected in the late morning or early afternoon from three
182 discrete depths: surface, 1m below surface, and 1m above the lake bottom. Those volumes were
183 then immediately combined to provide an integrated water-column sample. During 2016 the
184 water samples were collected using 5L Niskin bottles and in 2019 the water was collected via
185 peristaltic pump. Water samples were stored in polyethylene bottles inside insulated coolers at
186 ambient temperature for transport back to the NOAA Great Lakes Environmental Research
187 Laboratory in Ann Arbor, MI. Experiments were set up around 16:00 local time, which was 3 to
188 5 hours after collection. As described in the section below, measurement of colony velocities
189 began the day following collection.

190 At each site, water temperature was recorded from either a buoy thermistor (averaged
191 over 24 hours) or, for stations where no buoy was present, a temperature sensor deployed during
192 collection (CIGLR and NOAA GLERL, 2019). Photosynthetically active radiation (PAR) was
193 measured throughout the water column using a submersible instrument (Biospherical Instruments
194 Inc., QSP-2300) and the light extinction coefficient (m^{-1}) was estimated by regressing the natural
195 log of PAR against depth (m) (Weiskerger et al., 2018). More detailed descriptions of the
196 collection methods, locations, and environmental context have been published previously
197 ([dataset] Burtner et al., 2020; [dataset] CIGLR and NOAA GLERL, 2019). Environmental data
198 for each sampling event is provided in Table 1 and Supplementary Material Table S1.

199

200

201

202

203

204 2.3 Experimental setup

205 In order to simulate light intensity expected at different depths in the water column,
206 microcosms (acid-cleaned 2-liter borosilicate bottles) were filled with lake water and assigned to
207 different light treatments: ambient light intensity, 30% of ambient intensity, and 10% of ambient
208 intensity. Bottles designated for the ambient light treatment were not covered, but polyester neutral
209 light density films (LEE Filters, Hampshire, UK) were applied to others to achieve light levels of 30% (only
210 in 2019) and 10% of ambient (2016 and 2019). The bottles were then submerged upside down in an
211 outdoor incubation tank (0.5 m³) filled with water, which was exposed to sunlight through the open top.
212 Water within the tank was continuously recirculated via pumps and the water was maintained at lake
213 temperature using a thermostatic water bath (Cole Parmer, Polystat). Temperature within the
214 incubation tank was recorded at 10-minute intervals during the 2019 experiments using a temperature
215 logger (RBR Ltd.) and it was found to remain within 2°C of the target temperature. To quantify incident
216 light exposure within the tank, PAR was continuously recorded using an underwater spherical sensor (LI-
217 COR, LI-192 Underwater Quantum Sensor) and the mean of the 6-h period before sampling was used to
218 represent light exposure history.

219 2.4 *Microcystis* velocity and size measurements

220 *Microcystis* size and velocity were empirically measured during the day following collection, with
221 the morning measurements made approximately 16 hours after the start of the incubation in the
222 outdoor tanks. Sub-samples were collected for micro-cinematography in the morning (09:00 local time)
223 and afternoon (15:00). At each time point, the bottles were gently inverted several times to mix the
224 contents before pouring an aliquot of each sample into a 25 mL cuvette. The cuvette (10mm × 10mm
225 inner dimension × 305mm tall, Friedrich & Dimmock, Inc.) was housed inside a thermal water jacket
226 (140mm × 140mm inner dimension × 400mm tall) that was placed inside a temperature-controlled room
227 matching ambient lake temperature at time of collection. A transparent ruler with mm graduations was

228 placed inside the thermal water jacket to allow for calibration between each set of recordings. The
229 micro-cinematography apparatus was located inside the temperature-controlled room and consisted of
230 a camera mounted on a 3D positioning frame that was controlled from the outside of the room via
231 joystick, allowing for the user to focus and move the camera system along the cuvette (Bundy et al.,
232 1998; Gill et al., 2017 their Fig 2.5). In contrast to the Schlieren system used by Bundy et al. (1998) and
233 Rowe et al. (2016) the present study used a shadowgraph optics system (Rasenat et al., 1989; Trainoff
234 and Cannell, 2002) with a laser light source (400-710nm, Stocker Yale Canada Inc., LASIRISTM) and a
235 digital video camera (Basler acA1300 – 60g mNIR) with image capturing software (Contemplas, GmbH,
236 Germany). The shadowgraph system allowed visualization of *Microcystis* colonies as small as 80 µm in
237 diameter. We verified accurate measurement of buoyant velocities in the system by measuring the
238 known buoyant velocities of 50 and 100 µm polystyrene microspheres (Gill et al., 2017).

239 A minimum of ten video segments were captured at each timepoint, taken at discrete
240 points along the length of the cuvette. Following video recording, *Microcystis* colonies were
241 identified by morphology and buoyant velocities were estimated using the motion analysis
242 software Vicon Motus (Contemplas, GmbH, Germany). Simultaneously with acquiring the
243 buoyant velocities, we assigned identities to colonies in calibrated image stills from Vicon Motus
244 and were then imported into ImagePro Insight (Media Cybernetics) to estimate colony size by
245 equivalent spherical diameter (ESD). ESD of an irregularly shaped object is the diameter of a
246 sphere of equivalent volume. In this case, the ESD was estimated by converting the projected
247 area of a *Microcystis* colony image to a diameter of a circle of equivalent area. Sizes were then
248 paired with each colony's corresponding velocity data. Velocity and size data were acquired for
249 a minimum of 20 (2016) or 26 (2019) colonies from each combination of experiment, light
250 intensity and time of day. In total, size and velocity were estimated for 729 individual colonies in

251 2016 and 1,522 colonies in 2019. Hereafter we refer to the estimated velocity and estimated
252 colony size as velocity and size, respectively.

253 The relationship between colony size and velocity (either positive or negative) is expected to
254 follow Stokes' law (Reynolds, 1973), where the force of gravity on a colony balances with the fluid drag
255 force when the colony reaches its terminal velocity.

256
$$V = \frac{g \Delta \rho D^2}{18 \varphi \mu} \quad (\text{Equation 1})$$

257 In Equation 1, V is the colony velocity (m s^{-1}), g is the gravitational acceleration constant (9.81 m s^{-2}), μ is
258 the viscosity of water (Pascal-second), D is the diameter of the colony (m), φ is the shape coefficient,
259 and $\Delta \rho$ is the difference in density between the water and the colony ($\rho_{\text{water}} -$
260 ρ_{colony} , kg m^{-3}) (Reynolds et al., 1987). The density of water at 22.5°C , the approximate average
261 temperatures across experiments, was estimated at 997.6557 kg/m^3 using the package 'marelac' in the
262 R statistical programming platform. If g , ρ_{water} , and μ are known, and φ is set to 1, Equation 1 can be
263 solved to estimate apparent colony density, an estimated parameter, using empirical buoyant or sinking
264 velocity observations and size measurements from a colony (Li et al., 2016; Reynolds et al., 1987).

265
$$\rho_{\text{colony}} = \rho_{\text{water}} - \frac{18 \varphi \mu V}{g D^2} \quad (\text{Equation 2})$$

266 In Equation 2, ρ_{water} is the density of freshwater and ρ_{colony} is apparent colony density (kg/m^3). Because
267 this method assumes that the shape factor is constant, apparent colony density represents not only the
268 density of a colony but also potential differences in shape or structure that influence velocity.

269

270

271 2.5 Statistical analyses

272 The effects of treatments on observed velocity and apparent colony density were analyzed by
273 fitting hierarchical linear models separately for each lake and year. The models included population-
274 level effects of light intensity (10%, 30% and ambient) and time of day (morning, afternoon) in complete
275 factorial and with their interaction. We distinguished between large and small colonies using the
276 approximate median size of 200 μm equivalent spherical diameter. To evaluate whether our findings
277 were sensitive to the size used for distinguishing large and small colonies, we repeated our analyses
278 using a size cutoff of 150 μm or 250 μm (Supplementary Materials Figures S1-S2). Each model also
279 included group-level effects, allowing the intercept and the population-level effects to vary among
280 stations and dates. The 'leave one out' information criterion was used to compare models with and
281 without each interaction or grouping term (Gelman et al., 2013). When those terms did not improve the
282 information criterion they were omitted.

283 All statistical analyses were performed within the R statistical platform. Models were fitted in a
284 Bayesian framework using a Gaussian error distribution and priors with a mean of zero and standard
285 deviation of 5. The package 'brms' (Bürkner, 2017) was used to compile and execute the Hamiltonian
286 Markov Chain Monte Carlo algorithm in the 'stan' language (Carpenter et al., 2017). Each model was
287 fitted in four separate Monte Carlo chains, each with 1,000 warm up iterations and 1,000 sampling
288 iterations. Adequate mixing of the chains was confirmed using the r-hat statistic, which was less than
289 1.01 in all cases. We assessed the fit of each model containing a continuous predictor using a Bayesian
290 R-squared (Gelman et al., 2018) and checked for influential observations using leave-one-out cross-
291 validation. The effects were tabulated directly from the pooled posterior distributions. The mean
292 posterior value was used as the estimate and the 2.5% and 97.5% quantiles as the credible interval (CI).
293 Select contrasts within each model were assessed using an evidence ratio (ER), or the ratio of the
294 number of posterior samples consistent with the hypothesis to the number of posterior samples

295 opposing the hypothesis. While an arbitrary cutoff was not used for evidence ratios (i.e. a threshold p-
296 value, Wasserstein et al., 2019), contrasts with ER below 5 were interpreted as having little support.
297 Estimates of mean velocities and densities from the models are listed in Supplementary Material Table
298 S2.

299

300 **3. Results**

301 **3.1 Effects of light intensity and time of day on observed velocities in Saginaw Bay**

302 Figure 1 (A, B) shows that the mean observed velocity of colonies from Saginaw Bay was
303 negative for each experiment and ranged from -30 to $-71 \mu\text{m s}^{-1}$ among the treatment combinations.
304 The light treatments behaved similarly in morning and afternoon and so the final model for Saginaw Bay
305 did not include an interaction between light intensity and time of day. In the July experiment the mean
306 observed colony velocity was similar across all treatment combinations and differed by only $13 \mu\text{m s}^{-1}$.
307 Compared to the experiment performed in July, colonies were more responsive to light intensity and
308 time of day in August. For the experiment performed in August, observed velocities were similar in the
309 10% and ambient light intensity treatments, but the 30% light intensity had velocities that were less
310 negative (ER= 51). In the August experiment the observed velocities were also less negative in the
311 morning than afternoon (ER= 17).

312

313

314

315

316 3.2 Effects of light intensity and time of day on observed velocities in western Lake Erie

317 Figure 1 (C, D) shows that *Microcystis* colonies from western Lake Erie in 2019 were more often
318 positively buoyant compared to Saginaw Bay and that their observed velocity was more responsive to
319 light intensity and duration. This pattern was apparent in the morning of each experiment, but the
320 difference in observed velocities between the morning 10% and ambient light intensities were greater in
321 July ($59\text{-}149 \mu\text{m s}^{-1}$, $\text{ER}>4,000$) than in August ($0.8\text{-}25 \mu\text{m s}^{-1}$, $\text{ER}= 22$). Unlike the monotonic effect of
322 light intensity observed in the morning, in both experiments the afternoon 10% light intensity treatment
323 showed positive buoyancy whereas the 30% and ambient treatments exhibited negative buoyancy ($\text{ER}>$
324 1,300). Within each light intensity treatment, the colonies were consistently less buoyant in afternoon
325 compared to the morning.

326 Figure 1 (E) shows that the *Microcystis* colonies from western Lake Erie were both more buoyant
327 and more variable in 2016 than in 2019. The model for the 2016 experiments did not include an
328 interaction between light intensity and time of day. In 2016, colonies were more positively buoyant at
329 10% light intensity than at ambient light intensity ($\text{ER} = 147$). While these effects of light intensity and
330 time of day were largely consistent among the experiments (Figure 1 E), the mean velocities in each
331 combination of treatments varied among locations and dates. In each experiment the mean velocities
332 were positive for both light intensity treatments during the morning and the 10% treatment in the
333 afternoon. In the afternoon the ambient light treatment's CI overlapped zero for five out of seven
334 experiments.

335

336

337

338 3.3 Relationships between observed buoyant velocity, size, and apparent colony density

339 Previous studies have shown that colony size is a particularly influential determinant of buoyant
340 velocity in natural populations of *Microcystis* (Nakamura et al., 1993; Reynolds, 1973). For spherical
341 particles following Stokes' Law, the relationship between size and velocity follows a power function,
342 which means that buoyant or sinking velocities should increase proportionally to the square of colony
343 diameter (Reynolds, 1987). Given this expected relationship between size and velocity, a regression of
344 log velocity versus log size should have a positive slope equal to 2 for spherical colonies of uniform
345 density. Figure 2 shows that in Saginaw Bay the relationship between observed velocity and estimated
346 colony size, was negative and the slope for both positively buoyant (mean slope = -0.73, CI -0.18 to -
347 1.31) and sinking colonies (mean slope= -0.45, CI -0.18 to -0.70) was low and the fit of the prescribed
348 relationship was weak for both sinking and floating colonies (R^2 = 0.03 and 0.06, respectively).
349 The experiments from 2019 in Lake Erie showed weak positive relationships between estimated colony
350 size and observed buoyant velocity (mean slope = 0.41, CI 0.08 to 0.24, R^2 = 0.29) and between
351 estimated size and observed sinking velocity (mean slope= 0.42, CI 0.20 to 0.64, R^2 = 0.08, Figure
352 2). Figure 3 shows that apparent colony density was not correlated with estimated size, but the variance
353 in apparent colony density decreased dramatically with estimated colony size in both lakes. This pattern
354 was also evident in each experiment and within light intensity treatments.

355 3.4 Response of colony density to treatments in Saginaw Bay

356 Figure 4 shows that the mean apparent colony density in Saginaw Bay experiments was greater
357 than that of water, consistent with the observation that those colonies tended to sink. In the July
358 experiment from Saginaw Bay the mean apparent colony density was similar between large ($>200 \mu\text{m}$
359 ESD) and small colonies, but in August the apparent colony density was consistently greater for small
360 colonies than large colonies (ER> 4000).

361 3.5 Response of colony density in western Lake Erie

362 Unlike colonies from Saginaw Bay, large and small *Microcystis* colonies from western Lake Erie
363 showed different responses to light intensity and time of day. Figure 4 (C, D) shows that small colonies
364 were more responsive to light intensity in western Lake Erie. In morning, the difference in apparent
365 colony density between the 10% and ambient light intensity treatments was 1.97 (July) and 0.36 kg m⁻³
366 (August) for large colonies, but the difference was 4.75 (July) and 2.32 kg m⁻³ (August) in the smaller
367 colonies. The interaction among estimated colony size, light intensity treatment, and time of day also
368 means that the difference in apparent colony density between large and small colonies depends on both
369 the light intensity and duration. Under 10% ambient light intensity, small colonies had lower apparent
370 colony density than large colonies in morning (ER >4000) and in the afternoon (ER= 500 in July, 5.5 in
371 August). Under 30% light intensity, small colonies were less dense than large colonies in morning
372 (ER=1330 in July, 2.4 in August) and more dense in the afternoon (ER= 2.2, 16.5). Those patterns were
373 similar in the ambient light treatment where small colonies were less dense in the morning (ER= 50 in
374 July, 2.5 in August) and more dense in the afternoon (ER= 7.9, 30).

375

376 **4. Discussion**

377 4.1 Effects of light intensity and time of day on buoyancy

378 Consistent with previous studies on buoyant movement by *Microcystis* colonies, this study
379 provides support for the hypothesis that increased light intensity makes colonies less buoyant. All of the
380 experiments from western Lake Erie were consistent with the observations of buoyant regulation from
381 natural systems (Aparicio Medrano et al., 2013; Reynolds, 1973; Zhu et al., 2014b) and experiments
382 (Konopka et al., 1987; Li et al., 2016; Thomas and Walsby, 1985). These short-term changes in buoyant
383 velocities can likely be attributed to the accumulation of carbohydrates under higher light intensities,

384 contributing to a lower observed positively buoyant velocity or negative velocities (Kromkamp and Mur,
385 1984; Visser et al., 1997). However, the two experiments from Saginaw Bay do not support the
386 hypothesis that increasing light intensity causes *Microcystis* colonies to become less buoyant and,
387 moreover, do not suggest that increasing light intensity makes colonies sink more quickly.

388 4.2 Relationship between buoyant observed velocity and size

389 Figure 2 shows that the slope of log observed colony velocity versus log size is smaller than
390 previous studies. Nakamura et al (1993) proposed that a slope of 1.5 is appropriate owing to the
391 presence of voids within 'floc-type' colonies. The slopes estimated for both western Lake Erie and
392 Saginaw Bay were less than 1, suggesting that the colonies likely have voids and structure that influence
393 their movement. The same regression model was fitted to 15 published datasets from other studies
394 (Supplementary Material Tables S3 and S4), which had a population-level mean slope of 1.03 (CI 0.77 to
395 1.29) for buoyant colonies and a mean slope of 0.77 for sinking colonies (CI 0.43 to 1.17). Moreover, the
396 slopes for those individual studies were higher than those observed in either western Lake Erie or
397 Saginaw Bay. The contradictory relationship between colony size and velocity in Saginaw Bay and the
398 weak relationship found in western Lake Erie both suggest that the density of the colonies may not be
399 independent of their size. A similar pattern was reported previously (Li et al., 2016) and could reflect
400 differences in colony density with size or differences in structure and shape of large versus small
401 colonies (Zhang et al., 2007; Zhu et al., 2014a). Regarding colony structure and shape, general
402 differences in colony morphology were observed between larger and smaller colonies. The larger
403 colonies observed often had large voids in their colony shape, whereas smaller colonies consisted of
404 cells more densely packed aggregates of cells (Figure 5).

405

406

407 4.3 Colony density and size

408 Apparent colony densities were not correlated with colony size (Figure 3). The decreased
409 variance in density and size among large *Microcystis* colonies may be explained by the observation that
410 small colonies are mostly packed aggregates of cells, whereas larger colonies tend to have voids among
411 their mucilage and cells (Figure 5, Nakamura et al., 1993). Thus, larger colonies should have a colony
412 density that is more similar to the density of water. A study by Li et al. (2016) found that density of
413 buoyant *Microcystis wesenbergi* and *M. ichthyoblabe* colonies increased linearly with colony size, but
414 that density of buoyant *M. aeruginosa* colonies was independent of size. The weak relationship between
415 colony density and colony size was attributed to the increased fraction of intercellular space in larger
416 colonies and also the influence of a relatively dense extracellular matrix (i.e., mucilage) in larger
417 colonies. Li et al. (2016) hypothesized that decreasing colony density and increasing colony size are
418 separate and non-exclusive means for *Microcystis* to regulate buoyancy and migrate vertically within the
419 water column. While Figure 3 does not show that colony density changes monotonically with colony
420 size, it does suggest that the apparent density of small versus large colonies could show differential
421 responses to light intensity and time of day. The model by Visser et al (1997) predicts that while all
422 colony sizes change their density in response to light intensity and duration, smaller colonies should
423 exhibit more variable densities in response to light than large colonies. This prediction is partially
424 supported by the patterns shown in Figure 4, although in the present study the largest colonies (> 200
425 μm ESD) exhibited little variation in apparent colony density.

426 4.4 Response of apparent colony density to light

427 The absence of discernible effects of light intensity on apparent colony density in Saginaw Bay is
428 expected given the lack of consistent effects of light intensity on velocity (Figures 2, 4). Similarly, the
429 greater mean apparent colony density in small colonies is expected from the relationship shown in
430 Figure 2. However, colonies from western Lake Erie did vary apparent colony density in response to light

431 intensity and time of day, particularly among the smaller colonies. The pattern of greater density change
432 in smaller colonies is consistent with the prediction from some models (Visser et al., 1997; Wallace and
433 Hamilton, 1999) and has been suggested as a mechanism by which small colonies can avoid the
434 damaging effect of high light intensities, whereas larger colonies are able to achieve sufficient velocities
435 for migration using smaller changes in colony density (Xiao et al., 2012). A complementary explanation
436 for this pattern is that larger colonies tend to have voids between the cells and mucilage (Li et al., 2016;
437 Nakamura et al., 1993), which serves to minimize the effect of changes in cell density on colony density.
438 While small versus large colonies showed different responses in density, the net effect in terms of
439 vertical migration and vertical distribution of biomass depends on the combined effect of density and
440 colony size (and also shape). Importantly, vertical divergence of colony sizes within the water column
441 (Aparicio Medrano et al., 2013; Zhu et al., 2014b) can potentially lead to different colony density in small
442 versus large colonies at the same time of day (Chien et al., 2013).

443 **4.5 Differences in buoyancy behavior between Saginaw Bay and western Lake Erie**

444 The experiments found dramatic differences in buoyancy behavior between the two lakes
445 (Figures 1, 4). Although there has not been a systematic comparison of buoyancy characteristics in
446 populations from different lakes, several environmental factors are known to play a role in regulating
447 buoyancy in *Microcystis*. As described previously, light intensity and duration are predominant drivers of
448 changes in buoyancy. While the lakes are at similar latitude and receive comparable incident radiation,
449 the attenuation of light within the water was more rapid in western Lake Erie than in Saginaw Bay (Table
450 1). Phytoplankton living in a turbulent mixed layer experience a light exposure averaged over the mixed
451 layer. For the mean PAR attenuation in Saginaw Bay (0.75 m^{-1} , Table 1), PAR averaged over a 5-m water
452 column would be 26% of the surface value, compared to 11% for the same water column depth with the
453 mean PAR attenuation for Lake Erie (1.9 m^{-1} , Table 1). Thus, the *Microcystis* colonies that were sampled
454 from Saginaw Bay may have been acclimated to a greater light level than those sampled in Lake Erie.

455 Another important determinant of buoyant behavior is N and P limitation, which acts
456 secondarily or interactively with light intensity (Brookes and Ganf, 2001; Chu et al., 2007; Konopka et al.,
457 1987). Total P concentrations were consistently greater in the experiments from western Lake Erie than
458 those from Saginaw Bay (Supplementary Material Table S1), while dissolved inorganic N was similar or
459 greater in Saginaw Bay. The dissolved inorganic N:P ratio was several-fold higher in Saginaw Bay than
460 western Lake Erie (Supplementary Material Table S1) and the seston C:P and N:P ratios in Saginaw Bay
461 (Figure 6) suggest potential for strong P limitation (Guildford and Hecky, 2000; Healey and Hendzel,
462 1979). The lower P concentrations in Saginaw Bay could be responsible for decreased buoyancy,
463 although further experimentation would be required to directly test that hypothesis. Temperature is
464 also known to be important for buoyancy, with warmer temperatures favoring increased buoyancy
465 (Thomas and Walsby, 1986; You et al., 2018). The lake water and incubation temperatures varied little
466 between Saginaw Bay and western Lake Erie in 2019, but in 2016 two experiments were performed
467 when the water temperature was less than 20°C (Table 1). In those experiments (October 3 and 11, Fig
468 1) the colonies remained buoyant under each combination of light intensity and time of day, which
469 suggests that temperature was still adequate for this behavior.

470 Another explanation for the difference in buoyancy behavior between the two lakes, and among
471 different sizes of colonies within each lake, is physiological variation among *Microcystis* strains. The
472 capacity to regulate buoyancy varies among *Microcystis* strains (Li et al., 2016; Xiao et al., 2012) and has
473 a genetic basis (*gvp* gene) required for gas vesicle formation (Mlouka et al., 2004). Different strains can
474 have different gas vesicle production characteristics that vary with light intensity; for example, strains
475 that may not float at typical low lab culture light intensities may become buoyant at high light
476 intensities, while floating strains may sink at high light intensities (Xiao et al. 2012). Because these
477 blooms are not composed of a single strain (Meyer et al., 2017), further research will be necessary to
478 determine whether those populations have different buoyancy responses.

479 4.6 Conclusions

480 The results of this study show that overall, *Microcystis* colonies from western Lake Erie were
481 more positively buoyant than those from Saginaw Bay and increased in density in response to light,
482 similar to previous experiments and models. The lack of a response to light in Saginaw Bay might be
483 attributable to higher light intensities or strong P-limitation in that environment. These differences
484 between *Microcystis* populations in the two lakes will likely affect how HABs are transported throughout
485 each system by influencing their likelihood to manifest as floating scums on the surface of the lake, or
486 settling to the bottom, during periods of calm weather. These differences also have important
487 implications for the ability to monitor total HAB biomass from ocean color remote sensing methods,
488 which can only detect surface concentrations. An unexpected finding from these experiments is that
489 buoyant velocities were weakly correlated with colony size and that this was explained by greater
490 plasticity of colony density in small colonies despite the same environmental conditions. This pattern is
491 likely explained by the observation that smaller colonies tend to be more geometrically compact
492 whereas larger colonies develop more complex shapes that include intercellular spaces.

493

494 **Acknowledgments**

495 This work was supported by the Great Lakes Restoration Initiative (GLRI) and the Cooperative Science
496 and Monitoring Initiative (CSMI) through awards to NOAA GLERL. Support for P.A.D., S.H., and C.M.G.
497 was provided through the NOAA Cooperative Agreement with the Cooperative Institute for Great Lakes
498 Research (CIGLR) at the University of Michigan (NA17OAR4320152). We gratefully thank Tonghui Ming
499 who aided in sample collection and buoyancy measurements in 2016, Russ Miller for help with
500 improving the function of the motor-drive and joystick for camera positioning, David Fanslow for help
501 with fabricating the sample column, and Timothy Maguire for his assistance within the R statistical

502 platform. This work is listed under GLERL contribution number: XXXX and CIGLR contribution number:
503 XXXX (*Will request number at proof correction step*).

504

505 Data availability statement

506 The complete dataset and annotated R code are provided as supplementary materials.

507

508 Author contributions

509 H.A.V., M.D.R, and C.M.G. designed the experiments. H.A.V. and J.R.S. designed and configured the
510 optics setup. P.A.D. and S.B.H. performed the experiments and analyses. All authors contributed to
511 analyzing the data and writing the manuscript and have approved the final article.

512 **References**

513 Aparicio Medrano, E., Uittenbogaard, R.E., Dionisio Pires, L.M., van de Wiel, B.J.H., Clercx, H.J.H., 2013. Coupling hydrodynamics and buoyancy regulation in *Microcystis aeruginosa* for its vertical distribution in lakes. *Ecological Modelling* 248, 41-56.

514

515

516 Bartlett, S.L., Brunner, S.L., Klump, J.V., Houghton, E.M., Miller, T.R., 2018. Spatial analysis of toxic or otherwise bioactive cyanobacterial peptides in Green Bay, Lake Michigan. *Journal*

517 of Great Lakes Research 44(5), 924-933.

518

519 Bertani, I., Obenour, D.R., Steger, C.E., Stow, C.A., Gronewold, A.D., Scavia, D., 2016. Probabilistically assessing the role of nutrient loading in harmful algal bloom formation in

520 western Lake Erie. *Journal of Great Lakes Research* 42(6), 1184-1192.

521

522 Bormans, M., Sherman, B., Webster, I., 1999. Is buoyancy regulation in cyanobacteria an adaptation to exploit separation of light and nutrients? *Marine and Freshwater Research*.

523 50(8), 897-906.

524

525 Bosse, K.R., Sayers, M.J., Shuchman, R.A., Fahnenstiel, G.L., Ruberg, S.A., Fanslow, D.L.,

526 Stuart, D.G., Johengen, T.H., Burtner, A.M., 2019. Spatial-temporal variability of in situ

527 cyanobacteria vertical structure in Western Lake Erie: Implications for remote sensing

528 observations. *Journal of Great Lakes Research* 45(3), 480-489.

529

530 Brookes, J.D., Ganf, G.G., 2001. Variations in the buoyancy response of *Microcystis aeruginosa* to nitrogen, phosphorus and light. *Journal of Plankton Research* 23(12), 1399-1411.

531

532 Bundy, M.H., Gross, T.F., Vanderploeg, H.A., Rudi Strickler, J., 1998. Perception of inert

533 particles by calanoid copepods: behavioral observations and a numerical model. *Journal of*

534 *Plankton Research* 20(11), 2129-2152.

534 Bürkner, P.-C., 2017. brms: An R package for Bayesian multilevel models using Stan. *Journal of*
535 *Statistical Software* 80(1), 1-28.

536 [dataset] Burtner, A., Kitchens, C., Fyffe, D., Godwin, C., Johengen, T., Stuart, D., Errera, R.,
537 Palladino, D., Fanslow, D., Gossiaux, D., 2020. Physical, chemical, and biological water
538 quality data collected from a small boat in Saginaw Bay, Lake Huron, Great Lakes from
539 2019-05-30 to 2019-10-03. NOAA National Centers for Environmental Information,
540 Accession number 0209220, <https://accession.nodc.noaa.gov/0209220>.

541 Carmichael, W.W., Boyer, G.L., 2016. Health impacts from cyanobacteria harmful algae
542 blooms: Implications for the North American Great Lakes. *Harmful Algae* 54, 194-212.

543 Carpenter, B., Gelman, A., Hoffman, M.D., Lee, D., Goodrich, B., Betancourt, M., Brubaker,
544 M., Guo, J., Li, P., Riddell, A., 2017. Stan: A probabilistic programming language. *Journal of*
545 *Statistical Software* 76(1).

546 Chaffin, J.D., Bridgeman, T.B., Heckathorn, S.A., Mishra, S., 2011. Assessment of *Microcystis*
547 growth rate potential and nutrient status across a trophic gradient in western Lake Erie.
548 *Journal of Great Lakes Research* 37(1), 92-100.

549 Chien, Y.C., Wu, S.C., Chen, W.C., Chou, C.C., 2013. Model simulation of diurnal vertical
550 migration patterns of different-sized colonies of *Microcystis* employing a particle trajectory
551 approach. *Environmental Engineering Science* 30(4), 179-186.

552 Chu, Z., Jin, X., Yang, B., Zeng, Q., 2007. Buoyancy regulation of *Microcystis flos-aquae* during
553 phosphorus-limited and nitrogen-limited growth. *Journal of Plankton Research* 29(9), 739-
554 745.

555 [dataset] CIGLR and NOAA GLERL, 2019. Physical, chemical, and biological water quality
556 monitoring data to support detection of Harmful Algal Blooms (HABs) in western Lake Erie,

557 collected by the Great Lakes Environmental Research Laboratory and the Cooperative
558 Institute for Great Lakes Research since 2012. NOAA National Centers for Environmental
559 Information, accession number 0187718, <https://doi.org/10.25921/11da-3x54>.

560 Fishman, D.B., Adlerstein, S.A., Vanderploeg, H.A., Fahnstiel, G.L., Scavia, D., 2010.
561 Phytoplankton community composition of Saginaw Bay, Lake Huron, during the zebra
562 mussel (*Dreissena polymorpha*) invasion: A multivariate analysis. *Journal of Great Lakes*
563 *Research* 36(1), 9-19.

564 Fogg, G., Walsby, A., 1971. Buoyancy regulation and the growth of planktonic blue-green algae.
565 Internationale Vereinigung für Theoretische und Angewandte Limnologie: Mitteilungen
566 19(1), 182-188.

567 Gelman, A., Carlin, J.B., Stern, H.S., Dunson, D.B., Vehtari, A., Rubin, D.B., 2013. Bayesian
568 data analysis. CRC Press, Boca Raton Florida.

569 Gelman, A., Goodrich, B., Gabry, J., Vehtari, A., 2019. R-squared for Bayesian Regression
570 Models. *The American Statistician* 73(3), 307-309.

571 Gill, D., Ming, T., Ouyang, W., 2017. Improving the Lake Erie HAB Tracker: A Forecasting &
572 Decision Support Tool for Harmful Algal Blooms, Master's Capstone Project, School for
573 Natural Resources and Environment. University of Michigan.
574 <http://hdl.handle.net/2027.42/136562>

575 Guildford, S.J., Hecky, R.E., 2000. Total nitrogen, total phosphorus, and nutrient limitation in
576 lakes and oceans: Is there a common relationship? *Limnology and Oceanography* 45(6),
577 1213-1223.

578 Harke, M.J., Steffen, M.M., Gobler, C.J., Otten, T.G., Wilhelm, S.W., Wood, S.A., Paerl, H.W.,
579 2016. A review of the global ecology, genomics, and biogeography of the toxic
580 cyanobacterium, *Microcystis* spp. *Harmful Algae* 54, 4-20.

581 Healey, F.P., Hendzel, L.L., 1979. Indicators of phosphorus and nitrogen deficiency in five algae
582 in culture. *Journal of the Fisheries Research Board of Canada* 36(11), 1364-1369.

583 Hilborn, E.D., Fournie, J.W., 2008. Human Health Effects Workgroup Report, In: Hudnell, H.K.,
584 Lajtha, A., Paoletti, R. (Eds.), *Cyanobacterial harmful algal blooms: state of the science and*
585 *research needs*. Springer New York, New York, NY, pp. 579-606.

586 Hozumi, A., Ostrovsky, I., Sukenik, A., Gildor, H., 2019. Turbulence regulation of *Microcystis*
587 surface scum formation and dispersion during a cyanobacteria bloom event. *Inland Waters*
588 10(1), 51-70.

589 Huisman, J., Sharples, J., Stroom, J.M., Visser, P.M., Kardinaal, W.E.A., Verspagen, J.M.H.,
590 Sommeijer, B., 2004. Changes in turbulent mixing shift competition for light between
591 phytoplankton species. *Ecology* 85(11), 2960-2970.

592 Ibelings, B.W., Mur, L.R., Kinsman, R., Walsby, A., 1991a. *Microcystis* changes its buoyancy in
593 response to the average irradiance in the surface mixed layer. *Archiv für Hydrobiologie*
594 120(4), 385-401.

595 Ibelings, B.W., Mur, L.R., Walsby, A.E., 1991b. Diurnal changes in buoyancy and vertical
596 distribution in populations of *Microcystis* in two shallow lakes. *Journal of Plankton Research*
597 13(2), 419-436.

598 Johengen, T.H., Vanderploeg, H.A., Liebig, J.R., 2013. Effects of algal composition, seston
599 stoichiometry, and feeding rate on zebra mussel (*Dreissena polymorpha*) nutrient excretion

600 in two Laurentian Great Lakes, In: Nalepa, T.F., Schloesser, D.W. (Eds.), *Quagga and zebra*
601 mussels - biology, impacts, and control. CRC Press, Boca Raton, Florida, pp. 445-459.

602 Jöhnk, K.D., Huisman, J.E.F., Sharples, J., Sommeijer, B.E.N., Visser, P.M., Stroom, J.M., 2008.

603 Summer heatwaves promote blooms of harmful cyanobacteria. *Global Change Biology*
604 14(3), 495-512.

605 Konopka, A., Kromkamp, J.C., Mur, L.R., 1987. Buoyancy regulation in phosphate-limited
606 cultures of *Microcystis aeruginosa*. *FEMS Microbiology Ecology* 3(3), 135-142.

607 Kramer, E.L., 2018. Diel vertical distribution of *Microcystis* and associated environmental
608 factors in the western basin of Lake Erie. Master's Thesis, The University of Toledo, Toledo,
609 Ohio.

610 Kromkamp, J.C., Mur, L.R., 1984. Buoyant density changes in the cyanobacterium *Microcystis*
611 *aeruginosa* due to changes in the cellular carbohydrate content. *FEMS Microbiology Letters*
612 25(1), 105-109.

613 Li, M., Zhu, W., Guo, L., Hu, J., Chen, H., Xiao, M., 2016. To increase size or decrease density?
614 Different *Microcystis* species has different choice to form blooms. *Scientific Reports* 6,
615 37056.

616 Litchman, E., Klausmeier, C.A., 2008. Trait-based community ecology of phytoplankton.
617 *Annual Review of Ecology, Evolution, and Systematics* 39(1), 615-639.

618 Meyer, K.A., Davis, T.W., Watson, S.B., Denef, V.J., Berry, M.A., Dick, G.J., 2017. Genome
619 sequences of lower Great Lakes *Microcystis* sp. reveal strain-specific genes that are present
620 and expressed in western Lake Erie blooms. *PLoS One* 12(10), e0183859.

621 Michalak, A.M., Anderson, E.J., Beletsky, D., Boland, S., Bosch, N.S., Bridgeman, T.B.,
622 Chaffin, J.D., Cho, K., Confesor, R., Daloğlu, I., 2013. Record-setting algal bloom in Lake

623 Erie caused by agricultural and meteorological trends consistent with expected future
624 conditions. Proceedings of the National Academy of Sciences, 201216006.

625 Mlouka, A., Comte, K., Castets, A., Bouchier, C., Tandeau de Marsac, N., 2004. The gas vesicle
626 gene cluster from *Microcystis aeruginosa* and DNA rearrangements that lead to loss of cell
627 buoyancy. Journal of Bacteriology 186(8), 2355-2365.

628 Nakamura, T., Adachi, Y., Suzuki, M., 1993. Flotation and sedimentation of a single *Microcystis*
629 floc collected from surface bloom. Water Research 27(6), 979-983.

630 Okada, M., Aiba, S., 1983. Simulation of water-bloom in a eutrophic lake—III. Modeling the
631 vertical migration and growth of *Microcystis aeruginosa*. Water Research 17(8), 883-893.

632 Okada, M., Aiba, S., 1986. Simulation of water-bloom in a eutrophic lake—IV Modeling the
633 vertical migration in a population of *Microcystis aeruginosa*. Water Research 20(4), 485-490.

634 Oliver, R.L., 1994. Floating and sinking in gas-vacuolate cyanobacteria. Journal of Phycology
635 30(2), 161-173.

636 Paerl, H.W., Fulton, R.S., 3rd, Moisander, P.H., Dyble, J., 2001. Harmful freshwater algal
637 blooms, with an emphasis on cyanobacteria. ScientificWorld Journal 1, 76-113.

638 Paerl, H.W., Hall, N.S., Calandrino, E.S., 2011. Controlling harmful cyanobacterial blooms in a
639 world experiencing anthropogenic and climatic-induced change. The Science of the Total
640 Environment 409(10), 1739-1745.

641 Paerl, H.W., Otten, T.G., 2013. Harmful cyanobacterial blooms: causes, consequences, and
642 controls. Microbial Ecology 65(4), 995-1010.

643 Rasenat, S., Hartung, G., Winkler, B., Rehberg, I., 1989. The Shadowgraph method in
644 convection experiments. Experiments in Fluids 7(6), 412-420.

645 Reynolds, C., 1973. Growth and buoyancy of *Microcystis aeruginosa* Kütz. emend. Elenkin in a
646 shallow eutrophic lake. Proceedings of the Royal Society of London. Series B. Biological
647 Sciences 184(1074), 29-50.

648 Reynolds, C., Walsby, A., 1975. Water-blooms. Biological Reviews 50(4), 437-481.

649 Reynolds, C.S., 1987. Cyanobacterial water-blooms. Advances in Botanical Research Volume
650 13, pp. 67-143.

651 Reynolds, C.S., Oliver, R.L., Walsby, A.E., 1987. Cyanobacterial dominance: The role of
652 buoyancy regulation in dynamic lake environments. New Zealand Journal of Marine and
653 Freshwater Research 21(3), 379-390.

654 Ross, O.N., Sharples, J., 2004. Recipe for 1-D Lagrangian particle tracking models in space-
655 varying diffusivity. Limnology and Oceanography: Methods 2(9), 289-302.

656 Rowe, M., Anderson, E., Wynne, T.T., Stumpf, R., Fanslow, D., Kijanka, K., Vanderploeg, H.,
657 Strickler, J., Davis, T., 2016. Vertical distribution of buoyant *Microcystis* blooms in a
658 Lagrangian particle tracking model for short-term forecasts in Lake Erie. Journal of
659 Geophysical Research: Oceans 121(7), 5296-5314.

660 Stumpf, R.P., Wynne, T.T., Baker, D.B., Fahnenstiel, G.L., 2012. Interannual variability of
661 cyanobacterial blooms in Lake Erie. PLoS One 7(8), e42444.

662 Tang, H., Vanderploeg, H.A., Johengen, T.H., Liebig, J.R., 2014. Quagga mussel (*Dreissena*
663 *rostriformis bugensis*) selective feeding of phytoplankton in Saginaw Bay. Journal of Great
664 Lakes Research 40, 83-94.

665 Thomas, R., Walsby, A., 1985. Buoyancy regulation in a strain of *Microcystis*. Microbiology
666 131(4), 799-809.

667 Thomas, R., Walsby, A., 1986. The effect of temperature on recovery of buoyancy by
668 *Microcystis*. *Microbiology* 132(6), 1665-1672.

669 Trainoff, S.P., Cannell, D.S., 2002. Physical optics treatment of the Shadowgraph. *Physics of*
670 *Fluids* 14(4), 1340-1363.

671 Vanderploeg, H.A., Liebig J.R., Carmichael W.W., Agy M.A., Johengen T.H.,
672 Fahnenstiel G.L., and Nalepa T.F., 2001. Zebra mussel (*Dreissena polymorpha*) selective
673 filtration promoted toxic *Microcystis* blooms in Saginaw Bay (Lake Huron) and Lake Erie.
674 *Canadian Journal of Fisheries and Aquatic Sciences* 58(6), 1208-1221.

675 Vanderploeg, H. A., Nalepa T.F., Jude D.J., Mills E.L., Holeck K.T., Liebig J. R.,
676 Grigorovich I. A., and Ojaveer H., 2002. Dispersal and emerging ecological impacts of
677 Ponto-Caspian species in the Laurentian Great Lakes. *Canadian Journal of Fisheries and*
678 *Aquatic Sciences* 59(7), 1209-1228.

679 Vanderploeg, H. A., Johengen T. H., and Liebig J. R., 2009. Feedback between zebra mussel
680 selective feeding and algal composition affects mussel condition: did the regime changer pay
681 a price for its success? *Freshwater Biology* 54(1), 47-63.

682 Visser, P.M., Ibelings, B.W., Mur, L.R., 1995. Autunmal sedimentation of *Microcystis* spp. as
683 result of an increase in carbohydrate ballast at reduced temperature. *Journal of Plankton*
684 *Research* 17(5), 919-933.

685 Visser, P.M., Ketelaarsl, H.A., van Breemen, L.W., Mur, L.R., 1996. Diurnal buoyancy changes
686 of *Microcystis* in an artificially mixed storage reservoir. *Hydrobiologia* 331(1-3), 131-141.

687 Visser, P.M., Passarge, J., Mur, L.R., 1997. Modelling vertical migration of the cyanobacterium
688 *Microcystis*. *Hydrobiologia* 349(1-3), 99-109.

689 Wallace, B.B., Bailey, M.C., Hamilton, D.P., 2000. Simulation of vertical position of buoyancy
690 regulating *Microcystis aeruginosa* in a shallow eutrophic lake. *Aquatic Sciences* 62(4), 320-
691 333.

692 Wallace, B.B., Hamilton, D.P., 1999. The effect of variations in irradiance on buoyancy
693 regulation in *Microcystis aeruginosa*. *Limnology and Oceanography* 44(2), 273-281.

694 Wasserstein, R.L., Schirm, A.L., Lazar, N.A., 2019. Moving to a world beyond “ $p < 0.05$ ”. *The
695 American Statistician* 73(sup1), 1-19.

696 Watson, S.B., Miller, C., Arhonditsis, G., Boyer, G.L., Carmichael, W., Charlton, M.N.,
697 Confesor, R., Depew, D.C., Hook, T.O., Ludsin, S.A., Matisoff, G., McElmurry, S.P.,
698 Murray, M.W., Peter Richards, R., Rao, Y.R., Steffen, M.M., Wilhelm, S.W., 2016. The re-
699 eutrophication of Lake Erie: Harmful algal blooms and hypoxia. *Harmful Algae* 56, 44-66.

700 Weiskerger, C.J., Rowe, M.D., Stow, C.A., Stuart, D., Johengen, T., 2018. Application of the
701 Beer–Lambert model to attenuation of photosynthetically active radiation in a shallow,
702 eutrophic lake. *Water Resources Research* 54(11), 8952-8962.

703 Wu, H., Yang, T., Wang, C., Tian, C., Donde, O.O., Xiao, B., Wu, X., 2020a. Co-regulatory role
704 of *Microcystis* colony cell volume and compactness in buoyancy during the growth stage.
705 *Environmental Science and Pollution Research* 27(34), 42313-42323.

706 Wu, X., Yang, T., Feng, S., Li, L., Xiao, B., Song, L., Sukenik, A., Ostrovsky, I., 2020b.
707 Recovery of *Microcystis* surface scum following a mixing event: Insights from a tank
708 experiment. *The Science of the Total Environment* 728, 138727.

709 Wynne, T.T., Stumpf, R.P., Tomlinson, M.C., Schwab, D.J., Watabayashi, G.Y., Christensen,
710 J.D., 2011. Estimating cyanobacterial bloom transport by coupling remotely sensed imagery
711 and a hydrodynamic model. *Ecological Applications* 21(7), 2709-2721.

712 Xiao, M., Li, M., Reynolds, C.S., 2018. Colony formation in the cyanobacterium *Microcystis*.
713 Biological Reviews 93(3), 1399-1420.

714 Xiao, Y., Gan, N., Liu, J., Zheng, L., Song, L., 2012. Heterogeneity of buoyancy in response to
715 light between two buoyant types of cyanobacterium *Microcystis*. Hydrobiologia 679(1), 297-
716 311.

717 You, J., Mallory, K., Hong, J., Hondzo, M., 2018. Temperature effects on growth and buoyancy
718 of *Microcystis aeruginosa*. Journal of Plankton Research 40(1), 16-28.

719 Zhang, M., Kong, F., Tan, X., Yang, Z., Cao, H., Xing, P., 2007. Biochemical, morphological,
720 and genetic variations in *Microcystis aeruginosa* due to colony disaggregation. World
721 Journal of Microbiology and Biotechnology 23(5), 663-670.

722 Zhu, W., Dai, X., Li, M., 2014a. Relationship between extracellular polysaccharide (EPS)
723 content and colony size of *Microcystis* is colonial morphology dependent. Biochemical
724 Systematics and Ecology 55, 346-350.

725 Zhu, W., Li, M., Luo, Y., Dai, X., Guo, L., Xiao, M., Huang, J., Tan, X., 2014b. Vertical
726 distribution of *Microcystis* colony size in Lake Taihu: Its role in algal blooms. Journal of
727 Great Lakes Research 40(4), 949-955.

728 **Figures and Tables - Titles (bold) / Captions**

Collection date	Station	Station depth (m)	Surface water Temperature (°C)	Station PAR extinction coefficient (m ⁻¹)	PAR (μmol m ⁻² s ⁻¹)	
					Morning	Afternoon
8/29/16	WE4	8.7	25.7	1.22	197	865
9/6/16	WE8	5.1	24.8	2.54	182	1298
9/12/16	WE9	2.4	23.3	3.32	180	1474
9/19/16	WE13	8.9	23.0	1.39	86	1366
9/28/16	WE6	2.3	18.3	1.64	15	240
10/3/16	WE13	2.8	18.9	3.52	81	949
10/11/16	WE8	5.0	17.3	1.44	69	956
7/29/19	WE2	5.6	25.7	2.66	95	1933
8/12/19	WE2	5.8	24.8	1.69	39	1380
7/10/19	SB14	4.3	23.5	0.57	178	2186
8/6/19	SB14	4.3	24.2	0.92	154	2012

729 Table 1. **Summary of temperature and light data for experiments.** Station SB14 is in Saginaw Bay of

730 Lake Huron and stations WE2, WE4, WE8, WE9, and WE13 are in western Lake Erie. PAR is the mean of

731 measurements recorded over the 6 hours prior to each set of buoyancy measurements. Additional

732 chemical and biological parameters are provided in Appendix Table A1.

733 **Figure 1. Observed colony buoyant velocities by treatment.** Colony buoyant velocities in response to
734 light intensity treatments during the morning and afternoon, for experiments performed in Saginaw Bay
735 in 2019 (A,B), western Lake Erie in 2019 (C,D) and western Lake Erie in 2016 (E). Values above zero on
736 the vertical axis indicate positively buoyant (floating) colonies and values below zero indicate negatively
737 buoyant (sinking) colonies. Each color point represents a measurement for a single colony, the black
738 markers and whiskers represent the mean and credible interval from the hierarchical linear model.

739 Figure 2. **Observed colony velocity as a function of colony size.** Log-log plot of colony buoyant and
740 sinking velocities as a function of colony size, represented by (equivalent spherical diameter, ESD), for
741 2019 Saginaw Bay (A,B) and western Lake Erie (C,D) samples. Negative velocities for sinking colonies
742 were converted to their absolute values to display the relationship on a log scale. Each regression model
743 included a group-level intercept for each sampling date, but including group-level effects on the slope
744 did not improve the information criterion and thus those terms were not included.

745 Figure 3. **Estimated apparent colony density as a function of colony size.** Size is represented by
746 (equivalent spherical diameter, ESD) in 2019 Saginaw Bay (A) and western Lake Erie (B).

747 Figure 4. **Estimated apparent colony density by treatment.** Apparent colony density according to light
748 intensity treatment, time of day, and colony size for experiments performed in Saginaw Bay (A,B) and
749 Lake Erie (C,D). Points are the mean of the posterior draws from each model and the error bars denote
750 the CI. The final model for colony density in Saginaw Bay did not include any interactions, but the model
751 for western Lake Erie was improved by the inclusion of the interactions among light intensity treatment,
752 time of day, and colony size. Horizontal lines represent the density of freshwater at the temperature for
753 each experiment

754 Figure 5. ***Microcystis* colony microcinematography captures.** Microcinematography image capture of
755 *Microcystis* (circled in red) collected on July 30, 2019 from Lake Erie (A) and August 7, 2019 from
756 Saginaw Bay (B). Smaller colonies tend to have a more compact geometry whereas larger colonies
757 reveal more complex shapes with intercellular voids as they increase in size.

758

759

760 Figure 6. **Seston N:P and C:P stoichiometry in Lake Erie and Saginaw Bay.** Plot of seston N:P (A) and C:P
761 (B) stoichiometry for samples collected from western Lake Erie (n=9) and Saginaw Bay (n=2). Data from
762 Lake Erie are depicted as a box-whisker chart where the horizontal line denotes, the median, the ends of
763 the box are the 25th and 75th percentiles, the whiskers are the 5th and 95th percentiles, and points
764 represent outliers more than twice the interquartile distance from the median. Data from Saginaw Bay
765 are illustrated as discrete measurements. The inset dashed lines are indicators of P limitation proposed
766 by Healey and Hendzel 1979.

767

768

769

770

771

772

773

774

775

776

777

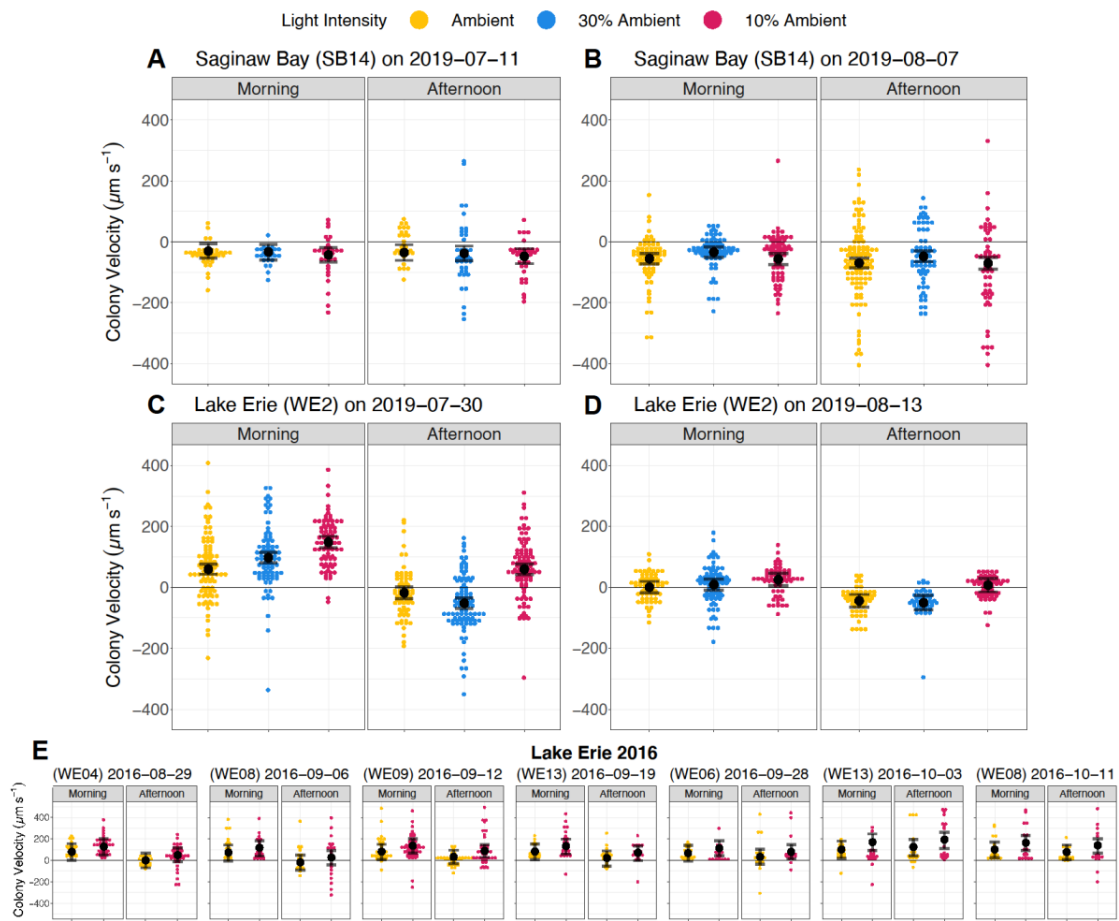
778

779

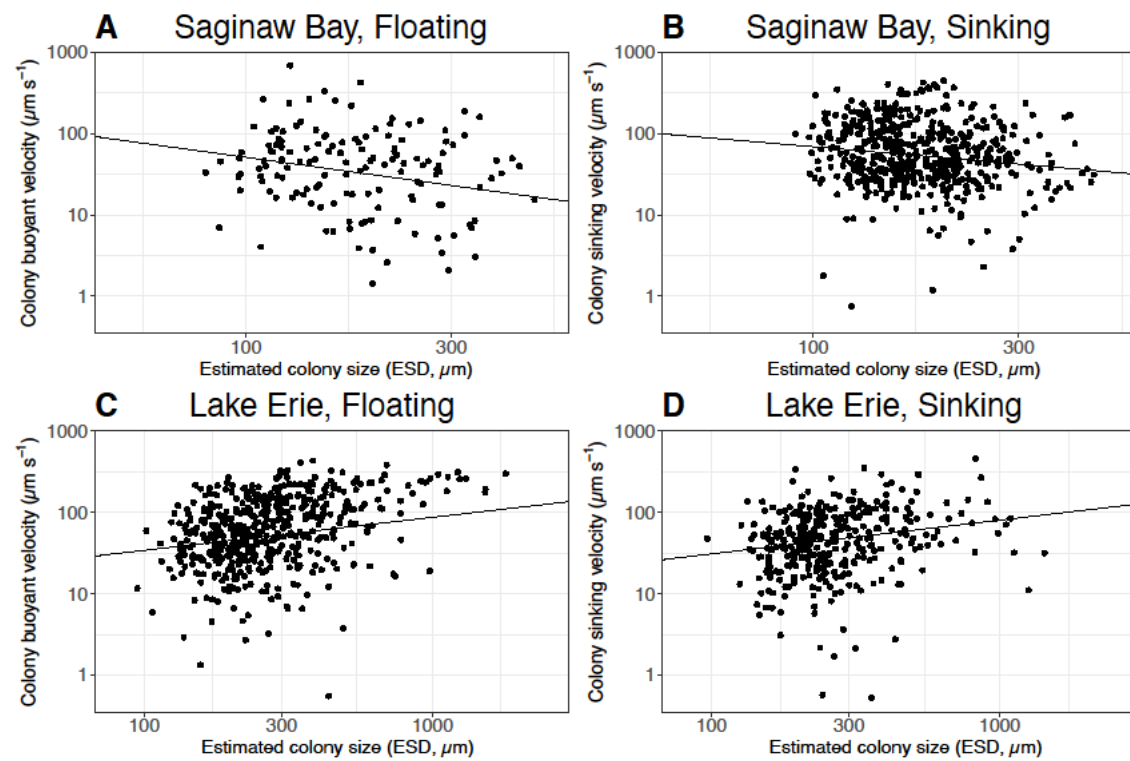
780

781

782



794 Figure2



795

796

797

798

799

800

801

802

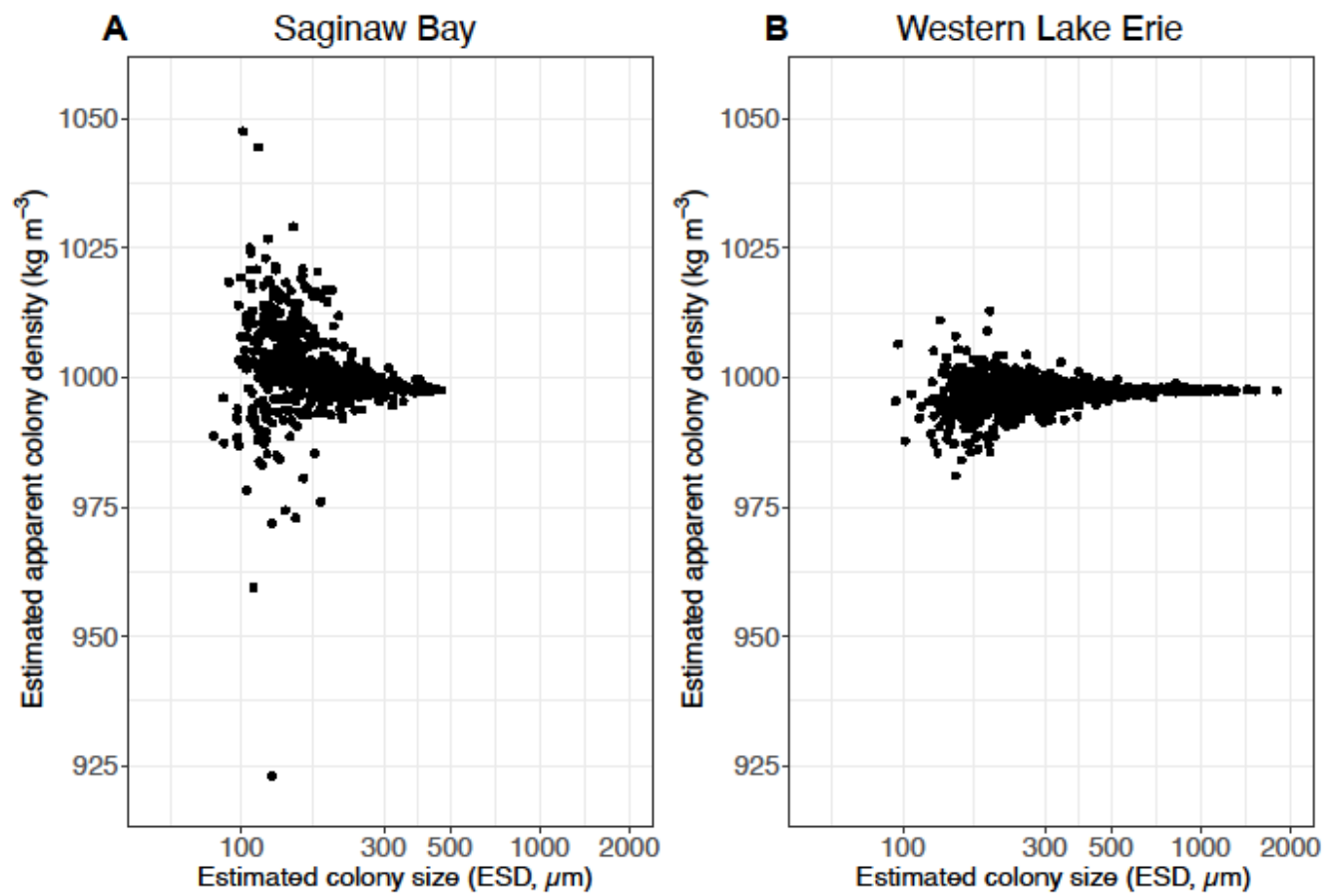
803

804

805

806

807

809
810

811

812

813

814

815

816

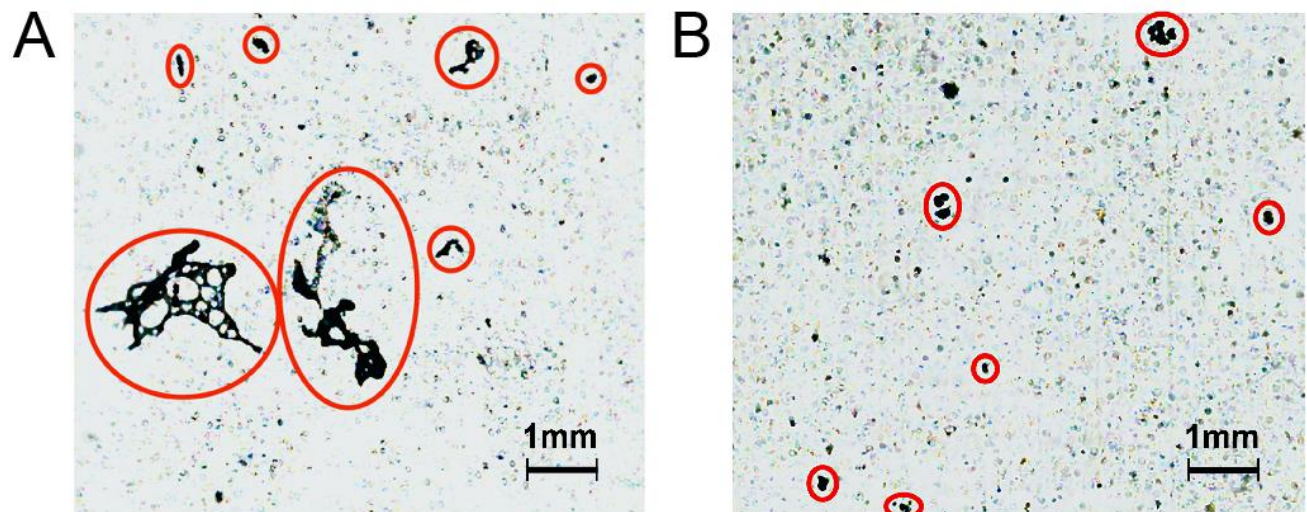
817

818

819



832 Figure5



833
834

835

836

837

838

839

840

841

842

843

844

845

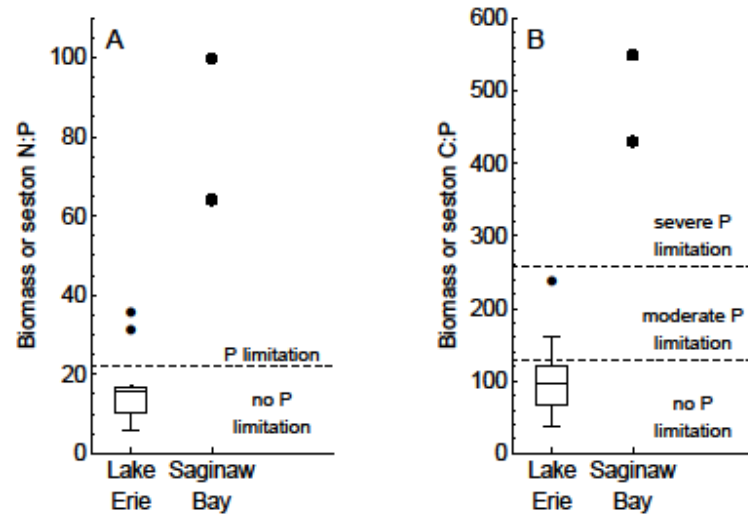
846

847

848

849

850 Figure6



851

852

853

854

855

856

857

858

859

860

861

862

863

864

865

866

867 **Declaration of interests**

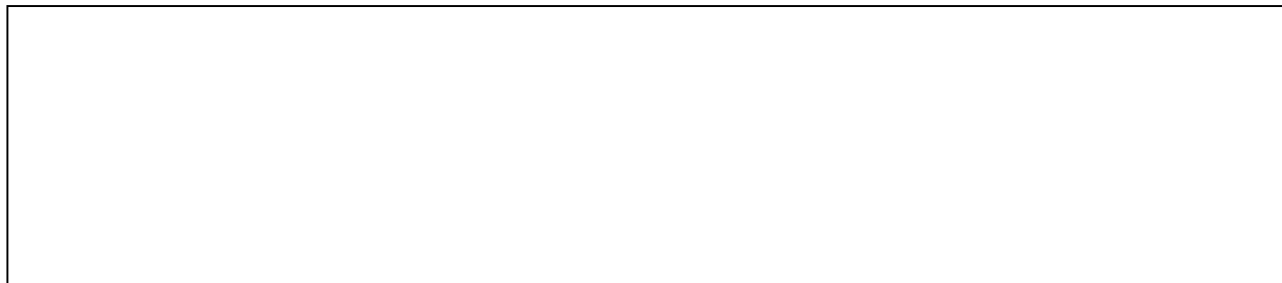
868

869 The authors declare that they have no known competing financial interests or personal relationships
870 that could have appeared to influence the work reported in this paper.

871

872 The authors declare the following financial interests/personal relationships which may be considered
873 as potential competing interests:

874



875

876

877

878

879

880

881

882

883

884

885

886

887

888

889

HARMFUL ALGAE

AUTHOR DECLARATION

Submission of an article implies that the work described has not been published previously (except in the form of an abstract or as part of a published lecture or academic thesis), that it is not under consideration for publication elsewhere, that its publication is approved by all authors and tacitly or explicitly by the responsible authorities where the work was carried out, and that, if accepted, it will not be published elsewhere in the same form, in English or in any other language, without the written consent of the copyright-holder.

By attaching this Declaration to the submission, the corresponding author certifies that:

- The manuscript represents original and valid work and that neither this manuscript nor one with substantially similar content under the same authorship has been published or is being considered for publication elsewhere.
- Every author has agreed to allow the corresponding author to serve as the primary correspondent with the editorial office, and to review the edited typescript and proof.
- Each author has given final approval of the submitted manuscript and order of authors. Any subsequent change to authorship will be approved by all authors.
- Each author has participated sufficiently in the work to take public responsibility for all the content.

1 **Highlights:**

2 • *Microcystis* colonies in western Lake Erie were mostly buoyant

3 • *Microcystis* colonies in Saginaw Bay were mostly sinking

4 • Buoyant and sinking velocities were weakly correlated with colony size

5 • Apparent colony density of small colonies was more variable and responsive to light

6

7

8

9

10

11

12

13

14

15

16

17

18

19

20

21

22

23

24